1521-0103/382/3/327–334$35.00
THE JOURNAL OF PHARMACOLOGY AND EXPERIMENTAL THERAPEUTICS

dx.doi.org/10.1124/jpet.122.001232
J Pharmacol Exp Ther 382:327–334, September 2022

Influence of Glutathione-S-Transferase A1*B Allele on the Metabolism of the Aromatase Inhibitor, Exemestane, in Human Liver Cytosols and in Patients Treated With Exemestane

Irina Teslenko, Julia Trudeau, Shaman Luo, Christy J.W. Watson, Gang Chen, Cristina I. Truica, and Philip Lazarus

Department of Pharmaceutical Sciences, College of Pharmacy and Pharmaceutical Sciences, Washington State University, Spokane, Washington (I.T., J.T., S.L., C.J.W.W., G.C., P.L.) and Penn State University, College of Medicine, Division of Hematology and Oncology, Department of Medicine, Hershey, Pennsylvania (C.I.T.)

Received March 21, 2022; accepted June 21, 2022

ABSTRACT

Exemestane (EXE) is used to treat postmenopausal women diagnosed with estrogen receptor positive (ER+) breast cancer. A major mode of metabolism of EXE and its active metabolite, 17β-dihydroexemestane, is via glutathionylation by glutathione-S-transferase (GST) enzymes. The goal of the present study was to investigate the effects of genetic variation in EXE-metabolizing GST enzymes on overall EXE metabolism. Ex vivo assays examining human liver cytosols from 75 subjects revealed the *GSTA1 *B*B* genotype was associated with significant decreases in S-(androsta-1,4-diene-3,17-dion-6α-ylmethyl)-L-glutathione ($P = 0.034$) and S-(androsta-1,4-diene-17β-ol-3-on-6α-ylmethyl)-L-gutathione ($P = 0.014$) formation. In the plasma of 68 ER+ breast cancer patients treated with EXE, the *GSTA1 *B*B* genotype was associated with significant decreases in both EXE-cysteine (cys) (29%, $P = 0.0056$) and 17β-DHE-cys (34%, $P = 0.032$) as compared with patients with the *GSTA1*A*A* genotype, with significant decreases in EXE-cys ($P_{trend} = 0.0067$) and 17β-DHE-cys ($P_{trend} = 0.028$) observed in patients with increasing numbers of the *GSTA1*B* allele. A near-significant ($P_{trend} = 0.060$) trend was also observed for urinary EXE-cys levels from the same patients. In contrast, plasma and urinary 17β-DHE-Gluc levels were significantly increased (36%, $P = 0.00097$ and 52%, $P = 0.0089$; respectively) in patients with the *GSTA1 *B*B* genotype. No significant correlations were observed between the GSTM1 null genotype and EXE metabolite levels. These data suggest that the *GSTA1*B* allele is associated with interindividual differences in EXE metabolism and may play a role in interindividual variability in overall response to EXE.

SIGNIFICANCE STATEMENT

The present study is the first comprehensive pharmacogenomic investigation examining the role of genetic variability in GST enzymes on exemestane metabolism. The GSTA1 *B*B genotype was found to contribute to interindividual differences in the metabolism of EXE both ex vivo and in clinical samples from patients taking EXE for the treatment of ER+ breast cancer. Since GSTA1 is a major hepatic phase II metabolizing enzyme in EXE metabolism, the GSTA1*B allele may be an important biomarker for treatment outcomes and toxicities.

Introduction

Breast cancer accounts for 30% of all malignancies in women and continues to be the leading cause of cancer-related death in women worldwide (Loibl et al., 2021). Additionally, over their lifetime, women in the United States have a greater than 12% chance of being diagnosed with breast cancer (Akram et al., 2017). Primarily because of earlier detection and more effective systemic treatments (Harbeck and Gnant, 2017; Jahan et al., 2021), a steady decrease in mortality has been observed since the 1970s; however, variability exists in patient clinical response and survival, suggesting a need for treatment optimization and implementation of pharmacogenomics to personalize current standards of care (Vianna-Jorge et al., 2013).

Endocrine therapy is a cornerstone for the systemic treatment of estrogen receptor positive (ER+) breast cancer (Zelnak and O'Regan, 2015). The two major classes of endocrine therapies for postmenopausal women are selective ER modulators [e.g., tamoxifen] and aromatase inhibitors [AIs; e.g., exemestane (EXE)] (Coombes et al., 2007). Although tamoxifen has been the

This work was supported by the Public Health Service, the National Institutes of Health National Cancer Institute, and the US Department of Health and Human Services [Grant 1R01-CA164366-01A1] (to P.L.).
An earlier version of this paper appears in Research Square under the DOI: 10.21203/rs.3.rs-1479213/v1.
dx.doi.org/10.1124/jpet.122.001232.

ABBREVIATIONS: 17β-DHE, 17β-dihydroexemestane; 17β-DHE-cys, 6-methylcysteinylandrosta-1,4-diene-17b-hydroxy-3-one; 17β-DHE-Gluc, 17β -hydroxy-EXE-17-O-b-D-glucuronide; 17β-DHE-GS, S-(androsta-1,4-diene-17β-ol-3-on-6α-ylmethyl)-L-gutathione; AI, aromatase inhibitor; cys, cysteine; EXE, exemestane; EXE-cys, 6-methylcysteinylandrosta-1,4-diene-3,17-dione; EXE-GS, S-(androsta-1,4-diene-3,17-dion-6α-ylmethyl)-L-glutathione; GSH, gamma-L-glutamyl-L-cysteinyl-glycine (glutathione); GST, glutathione-S-transferase; HLC, human liver cytosol; TEM, total exemestane metabolites; UGT, UDP-glucuronosyltransferase; UHPLC-MS, ultra-high pressure liquid chromatography-mass spectrometry.

standard of care for over 30 years, AIs are superior for both the treatment and prevention of ER+ breast cancer (Coombes et al., 2007; Kieback et al., 2010; Goss et al., 2011). Recently updated clinical practice guidelines from the American Society of Clinical Oncology suggest that postmenopausal women with lymph node positive ER+ breast cancer, as well as some high-risk women with lymph node negative breast cancer, should be offered an extended 10 years of AI therapy (Burstein et al., 2019).

EXE is a third generation steroidal AI that acts by inhibiting the aromatase enzyme encoded by the *CYP19A1* gene, thus preventing the conversion of androgens to estrogens (Campos, 2004). EXE binds irreversibly in the active site of aromatase, where it effectively inactivates the enzyme. Consequently, estrogen levels in the blood are reduced by 85%–95% (Campos, 2004; Kittaneh and Glück, 2011) and new aromatase must be generated before estrogen synthesis can be resumed (Kittaneh and Glück, 2011). De novo synthesis of aromatase takes on average 5 days after a single dose of EXE, therefore a relatively small dose of EXE (25 mg) can effectively inhibit this enzyme when taken long term (Kittaneh and Glück, 2011). EXE is also highly efficacious as an adjuvant treatment and prevention therapy, demonstrating a 65% reduction in the incidence of invasive breast cancer among high-risk postmenopausal women [5-year Gail risk score higher than 1.66%; (Goss et al., 2011)]. However, some efficacy studies have shown that only 46% of ER+ breast cancer patients responded to EXE treatment (Paridaens et al., 2003; Paridaens et al., 2008). Additionally, some women experience adverse events such as musculoskeletal arthralgia, joint pain, fatigue, and hot flashes, which can lead to treatment discontinuation (Henry et al., 2012). One possible explanation for interindividual variability in patient response may be differential EXE metabolism caused by genetic polymorphisms in key metabolizing enzymes.

EXE metabolism occurs through conversion to an active metabolite, 17β-dihydroexemestane (17β-DHE), via phase I enzymes including cytochromes P450, aldo-keto reductases, and carbonyl reductases (Kamdem et al., 2011; Platt et al., 2016; Peterson et al., 2017). 17β-DHE is further metabolized by phase II glucuronidation via UDP-glucuronosyltransferase (UGT) 2B17 (Sun et al., 2010; Luo et al., 2017). In addition, both EXE and 17β-DHE can be glutathionylated by glutathione-S-transferase (GST) enzymes, primarily GSTs A1 and M1 (Teslenko et al., 2021), with the resulting glutathione (GSH) conjugates further metabolized to cysteine conjugates by γ-glutamyl transferase and dipeptidases (Hinchman and Ballatori, 1994; Hayes et al., 2005; Luo et al., 2018). In postmenopausal patients with ER+ breast cancer, cysteine conjugates of EXE and 17β-DHE comprise 77% and 35% of the total urinary and plasma EXE metabolites, respectively, indicating that glutathionylation is a major metabolic pathway for EXE (Luo et al., 2018).

The GST superfamily of enzymes are highly polymorphic, and several GST variants have been linked to a greater risk of developing a variety of cancers as well as variability in drug toxicity, cancer resistance, and altered drug metabolism (Perera et al., 2002; Elhasid et al., 2010; Josephy, 2010; Allocati et al., 2018). Genetic variants in the GSTA1 and GSTM1 enzymes are associated with altered enzyme expression or catalytic activity, often resulting in altered drug metabolism and clinical outcomes. The *GSTA1* gene exhibits three well-characterized single nucleotide polymorphisms (SNPs) in high linkage disequilibrium in the promoter region (−567 T>G, −69 C>T, and −52 G>A), (Morel et al., 2002) resulting in the *GSTA1*A* and *GSTA1*B* alleles. The *GSTA1*B* allele has been linked to lower hepatic expression of GSTA1 and altered metabolism of certain medications (Hayes and Strange, 2000; Ansari et al., 2017). In Caucasian populations, the *GSTA1*B* allele has a minor allele frequency of 0.43–0.49 (Mikstacki et al., 2016; Michaud et al., 2019). Additionally, a polymorphic copy number variant of *GSTM1* has been identified (minor allele frequency of 0.48–0.57 in Caucasian populations) (Geisler and Olshan, 2001) and has been shown to influence drug metabolism (Lucafò et al., 2019b). Genetic variations in these two enzymes could potentially alter overall patient response and toxicities related to EXE treatment. The primary objective of this study was to investigate the effect of polymorphisms in *GSTA1* and *GSTM1* on both glutathione conjugation activity in human liver tissue and in the formation of major phase II metabolites found in the plasma and urine of patients taking EXE.

Materials and Methods

Chemicals and Materials. EXE was purchased from Sigma-Aldrich (St Louis, MO) and gamma-L-glutamyl-L-cysteinyl-glycine (glutathione; GSH) was obtained from Alfa Aesar (Haverhill, MA). Liquid chromatography-mass spectrometry (LC-MS) grade formic acid and acetonitrile were obtained from Thermo-Fisher Scientific (Waltham, MA), and LC-MS grade ammonium formate was purchased from Sigma-Aldrich (St Louis, MO). An Acquity UHPLC BEH C18 column (2.1 × 100 mm) was purchased from Waters (Milford, MA). Pooled human liver cytosol (HLC) was obtained from Xenotech (Kansas City, KS). Pierce BCA protein assay kits, PureLink Genomic DNA Isolation kits, TaqMan Copy Number Reference Assays (RNase P, Human; catalog #A30064), GSTM1 TaqMan Copy Number Variant Assays (catalog # 4400291), and GSTA1 TaqMan SNP Genotyping Assays (catalog # 4351374) were purchased from Thermo-Fisher Scientific. All other chemicals were purchased from Thermo-Fisher Scientific unless otherwise specified.

Human Liver Specimens. Normal adjacent human liver tissue specimens and corresponding genomic DNA samples were procured from the Tissue Procurement Core at the H. Lee Moffitt Cancer Center (Tampa, FL) from 75 patients undergoing hepatocarcinoma surgery (Coughtrie et al., 1987; Yokota et al., 1989). Tissues were flash frozen within 2 hours of removal. The majority of subjects (>90%, n = 70) were Caucasian, with 6% (n = 5) of Hispanic descent; 36% (n = 27) were female and the average age was 63 years. Cytosolic fractions were prepared from each tissue sample using differential centrifugation methods described previously (Dellinger et al., 2007; Ashmore et al., 2018) and stored at −80°C. All procedures involving tissue specimens have been approved by the H. Lee Moffitt Cancer Center's Institutional Review Board and are in compliance with assurances submitted to and approved by the US Department of Health and Human Services.

Clinical Study Subjects. A total of 132 postmenopausal women diagnosed with breast cancer at the Penn State Hershey Medical Center (Hershey, PA) were recruited for this study. The Penn State Institutional Review Board approved the study with informed consent obtained from all individuals and all specimens deidentified. The majority of the subjects (94%, n = 124) were Caucasian, and their age range was 35–89 years. All subjects were women who had ER+ tumors and agreed to orally ingest 25 mg of EXE daily for at least 28 days. Patients receiving EXE simultaneously with adjuvant chemotherapy, other adjuvant endocrine treatments, or chronic corticosteroid or megestrol acetate therapy were excluded from the study. Included as control subjects were 10 healthy volunteers (all Caucasian, ages 45–70 years) who were not taking EXE. On day 28 of the study, subjects were instructed to provide blood (10 cc) and urine (up to 50 ml) at a time point 4–6 hours after

taking their last daily EXE dose. Differential centrifugation (1300 *g* for 15 minutes) was performed to fractionate the whole blood; aliquots of plasma, buffy coat, and urine were stored at −80°C until analysis (Luo et al., 2017; Luo et al., 2018), with genomic DNA extracted from corresponding buffy coats using standard protocols as previously described (Luo et al., 2018).

Glutathione Activity Assays. Glutathione conjugation activity assays were performed with the cytosolic fraction (HLC) of the human liver specimens obtained from the H. Lee Moffitt Cancer Center. Reactions were performed in duplicate in a total volume of 25 μl, containing 1 μl of HLC protein, 100 mM potassium phosphate buffer, and 250 μM of either EXE or 17β-DHE (Platt et al., 2016). Preincubation at 37°C for 3 minutes was followed by the addition of 5 mM GSH to initiate the reaction (1 hour, 37°C). Reactions were quenched with a mixture of ice-cold acetonitrile (25 μl) and deuterium labeled S-(androsta-1,4-diene-3,17-dion-6α-ylmethyl)-L-glutathione (D_3-EXE-GS) and S-(androsta-1,4-diene-17β-ol-3-on-6α-ylmethyl)-L-gutathione (D_3-DHE-GS) internal standards (Teslenko et al., 2021). After thorough mixing by vortex and centrifugation at 16,100 *g* (10 minutes at 4°C), supernatants (10 μl) were transferred to glass vials containing 10 μl water. As a positive control, reactions using commercial pooled (50 subjects) HLC protein were performed. Negative control reactions contained all components except an enzyme source. GSH conjugate metabolites of EXE and 17β-DHE were quantified against standard curves with known concentrations of S-(androsta-1,4-diene-3,17-dion-6α-ylmethyl)-L-glutathione (EXE-GS) or 17β-DHE-GS. Chemical synthesis of the EXE-GS and 17β-DHE-GS standards were previously described (Teslenko et al., 2021). Rates of EXE-GS and 17β-DHE-GS conjugation were calculated in nmol·min^{-1}·mg cytosolic protein^{-1}. Total HLC protein concentration was determined via the Pierce BCA assay.

Ultra-High Pressure Liquid Chromatography-Mass Spectrometry Conditions for GS Conjugate Detection. A validated method for monitoring EXE-GS and 17β-DHE-GS conjugate formation was used to quantify GSH conjugates (Teslenko et al., 2021). Briefly, GSH conjugates were detected using an LC-MS system (Waters Acquity UHPLC/XEVO G2-S QToF) with analyte separation achieved using a UHPLC BEH C18 column (2.1 × 100 mm) with a flow rate of 0.4 mL per min, a column temperature of 35°C, and a sample temperature of 8°C. EXE-GS was detected using mobile phase A (5 mM ammonium formate and 0.01% formic acid) and mobile phase B (100% acetonitrile) under the following conditions: 0.5 minutes at 25% B, a liner gradient to 100% B from 0.5 to 4 minutes, maintenance at 100% B for 1.5 minutes, with a re-equilibration step for 2 minutes at the initial conditions. 17β-DHE-GS was detected using the same mobile phases A and B with the following gradient: 2 minutes at 20% B, a linear gradient to 100% B from 0.5 to 4 minutes, 1.5 minutes at 100% B, followed by re-equilibration to initial conditions for 2 minutes. The MS was operated in MS/MS mode monitoring EXE-GS (m/z 604.2692→297.184), D_3-EXE-GS (m/z 607.281→300.203), 17β-DHE-GS (m/z 606.2849→299.2) and D_3-17β-DHE-GS (m/z 609.3037→302.203).

Plasma and Urine Metabolites. Urine and plasma EXE and its major metabolites [17β-DHE, 17β -hydroxy-EXE-17-O-b-D-glucuronide (17β-DHE-Gluc), 6-EXE-cys, and 6-17β-DHE-cys] from 68 subjects taking EXE were identified and quantified as previously described (Luo et al., 2018). The quantification limit for EXE and the metabolites 17β-DHE, 17β-DHE-Gluc, 6-EXE-cys, and 6-17β-DHE-cys were as follows: 2.1, 1.6, 1.2, 0.7, and 7.2 nM, respectively, in plasma and 2.1, 1.6, 6.3, 1.5, and 7.2 nM, respectively, in urine. All subjects had plasma EXE levels that were higher than 3 nM. As the average plasma concentration of EXE 8 hours after ingestion was previously shown to be greater than 3 nM (Jannuzzo et al., 2004; Valle et al., 2005), this ensured compliance with study protocols (i.e., that subjects had taken EXE within 8 hours of blood and urine collection).

Genotype Analysis. Genomic DNA (20 ng) from either human liver specimens or whole blood was used for genotyping using real-time PCR and TaqMan probes according to the manufacturer's recommended protocols. *GSTA1* (*GSTA1*A* and *GSTA1*B*) genotyping was performed using the GSTA1 TaqMan SNP Genotyping Assay. The promoter region −69 C>T (rs3957356) SNP was investigated, as it has previously been demonstrated that this SNP is in high linkage disequilibrium with the −567 T>G and −52 G>A SNPs (Morel et al., 2002). To genotype the *GSTM1* deletion polymorphism, the TaqMan Copy Number Variant Assay was used in conjunction with the TaqMan Copy Number Reference Assay of the human RNase P gene. All genotyping reactions were performed in quadruplicate using a Bio-Rad CFX384 real-time PCR machine. CopyCaller software was used to analyze *GSTM1* copy number variation.

Statistical Analysis. Statistical analyses were performed using GraphPad Prism version 6.01 (GraphPad Software, San Diego, CA). Statistical analysis included the unpaired *t* test and the one-way ANOVA trend test.

Results

Glutathione Conjugate Formation Versus GST Genotype in Human Liver Specimens. EXE-GS and 17β-DHE-GS rates of formation were measured in HLC from 75 liver specimens as described above. Within this panel of HLC, the mean rates of EXE-GS and 17β-DHE-GS formation were 0.76 ± 0.27 nmol·min^{-1}·mg cytosolic protein^{-1} and 0.12 ± 0.028 nmol·min^{-1}·mg cytosolic protein^{-1}, respectively (Table 1). The rate of GS conjugate formation with EXE ranged from 0.16 to 1.44 nmol·min^{-1}·mg cytosolic protein^{-1} and with 17β-DHE from 0.062 to 0.23 nmol·min^{-1}·mg cytosolic protein^{-1}.

Genomic DNA corresponding to the 75 liver tissue specimens was genotyped for common *GSTA1* and *GSTM1* polymorphisms. The *GSTA1* locus was genotyped for the wild type *GSTA1*A* allele (−567T, −69C, and −52G) and the variant *GSTA1*B* allele (−567G, −69T, and -52A) (Morel et al., 2002; Coles and Kadlubar, 2005b; Suvakov et al., 2014). The panel contained 29 samples that were homozygous wild type *A*A, 35 samples that were heterozygous *A*B, and 11 that were homozygous polymorphic *B*B. The *GSTA1*B* minor allelic frequency (0.39) was close to reported frequencies in Caucasian populations (Mikstacki et al., 2016; Michaud et al., 2019) and *GSTA1* genotypes were in Hardy Weinberg equilibrium. Additionally, the *GSTM1* deletion polymorphism was genotyped, with *GSTM1* *0*0 corresponding to the null genotype with no functional copies and *GSTM1* *1*1 corresponding to a wild-type genotype with two functional copies. Five samples were wild type *1*1, whereas 35 specimens were homozygous null *0*0, and another 35 specimens were heterozygous *1*0. The minor allele frequency of the *GSTM1*0* allele of 0.70 in this population was higher than previously reported values in Caucasians (0.48–0.57) (Geisler and Olshan, 2001) and *GSTM1* genotypes were not in Hardy-Weinberg equilibrium.

There was a significant (P_{trend} = 0.025) decrease in EXE-GS formation with increasing numbers of the GSTA1*B allele, with a rate of 0.82 ± 0.27 nmol·min^{-1}·mg cytosolic protein^{-1} observed for specimens with the *A*A genotype, 0.76 ± 0.25 nmol·min^{-1}·mg cytosolic protein^{-1} observed for specimens with the *A*B genotype, and 0.61 ± 0.25 nmol·min^{-1}·mg

TABLE 1
Rate of EXE-GS and 17β-DHE-GS formation in HLC specimens

	Mean ± SD (nmol·min^{-1}·mg HLC protein^{-1})[a]	Range (nmol·min^{-1}·mg HLC protein^{-1})[a]
EXE-GS	0.76 ± 0.27	0.16–1.44
17β-DHE-GS	0.12 ± 0.28	0.062–0.23

SD, standard deviation.
[a] n = 75 HLC specimens.

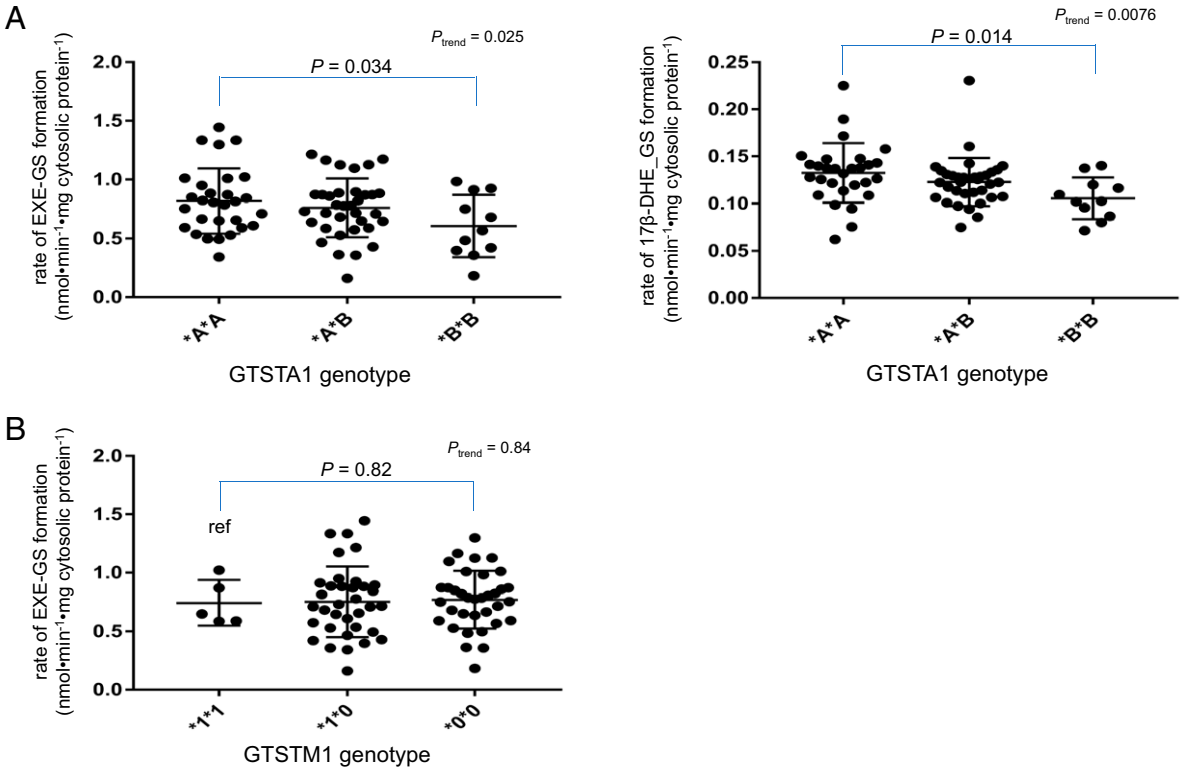

Fig. 1. Association between GST genotype and glutathione conjugate formation. The rate of EXE-GS and 17β-DHE-GS formation was examined in HLC from 75 normal human liver specimens and were stratified by *GSTA1* and *GSTM1* genotypes. Each individual dot represents the mean of two independent experiments. (A) EXE-GS and 17β-DHE-GS formation (nmol·min^{-1}·mg cytosolic protein^{-1}) versus *GSTA1* genotype. The *GSTA1*A* represents the wild type allele and *GSTA1*B* represents the polymorphic allele. (B) EXE-GS formation (nmol·min^{-1}·mg cytosolic protein^{-1}) versus *GSTM1* copy number variant. The *GSTM1*1* allele represents the wild-type gene, and the *GSTM1*0* allele corresponds to the *GSTM1* deletion variant. Since GSTM1 is not active against 17β-DHE, the 17β-DHE-GS conjugation rate versus *GSTM1* genotype was not included in this analysis. Within each genotype, the middle bars indicate the mean, whereas the upper and lower bars represent the standard error of the mean. Statistical analysis included unpaired t test and ANOVA test for trend.

cytosolic protein^{-1} observed for specimens with the *B*B genotype (Fig. 1A). The rates of 17β-DHE-GS formation showed a similarly significant (P_{trend} = 0.0076) decrease with increasing numbers of the GSTA1*B allele: 0.13 ± 0.032 nmol·min^{-1}·mg cytosolic protein^{-1} for specimens with the *A*A genotype, 0.12 ± 0.025 nmol·min^{-1}·mg cytosolic protein^{-1} for specimens with the *A*B genotype, and 0.11 ± 0.02 nmol·min^{-1}·mg cytosolic protein^{-1} for specimens with the *B*B genotype. Both EXE-GS and 17β-DHE-GS rates of formation were significantly lower (P = 0.034 and P = 0.014, respectively) for the *B*B genotype specimens as compared with the wild-type *A*A genotype specimens.

Since GSTA1 was the only enzyme previously shown to exhibit 17β-DHE-GS formation activity (Teslenko et al., 2021), only EXE-GS rates of formation were analyzed against the GSTM1 null genotype. After stratifying by GSTM1 genotype, no significant differences in EXE-GS formation were observed in the HLC from the same human liver specimens (Fig. 1B).

Phase II Plasma and Urine Metabolites Versus GST Genotype in Subjects Taking EXE. The levels of major phase II EXE metabolites in both plasma and urine are shown in Table 2. In plasma, the major phase II metabolites were 17β-DHE-Gluc (35% of total EXE metabolites), EXE-cys (32% of total EXE metabolites), and 17β-DHE-cys (9.5% of total EXE metabolites). A similar pattern was observed in urine, with EXE-cys, 17β-DHE-cys, and 17β-DHE-Gluc comprising 63%, 19%, and 16% of the total EXE metabolites, respectively.

The frequency of *GSTA1* genotypes in this population was 29% for *A*A subjects (n = 20), 46% for *A*B subjects (n = 31), and 25% for *B*B subjects (n = 17). The minor allele frequency of the *GSTA1*B* allele of 0.48 was, as expected, close to previously reported values in Caucasian populations (Mikstacki et al., 2016; Michaud et al., 2019) and in Hardy Weinberg equilibrium. *GSTM1* genotyping results indicated that 42 subjects exhibited the *GSTM1* null genotype (62%), 18 subjects had one copy of *GSTM1* (26%), whereas only six subjects had both copies present (9%). In addition, two subjects (3%) had three copies of the *GSTM1* gene. The minor allele frequency of the *GSTM1*0* allele of 0.78 in this population was higher than previously reported values in Caucasians (0.48–0.57) (Geisler and Olshan, 2001) and the GSTM1 genotypes were not in Hardy-Weinberg equilibrium.

The level of each plasma or urinary metabolite was expressed as a fraction of total exemestane metabolites (TEM). TEM included EXE and both phase I (17β-DHE) and phase II metabolites (17β-DHE-Gluc, EXE-cys, and 17β-DHE-cys). Subjects with the *GSTA1* *B*B genotype exhibited significantly lower relative levels of EXE-cys (P = 0.0056) and 17β-DHE-cys (P = 0.032) metabolites in plasma (0.25 EXE-cys/TEM and 0.073 17β-DHE-cys/TEM) as compared with those with the *GSTA1* *A*A genotype (0.35 EXE-cys/TEM and 0.11 17β-DHE-cys/TEM; Fig. 2A). The observed decreases corresponded to 29% for plasma EXE-cys levels and 34% for plasma 17β-DHE-cys levels. A significant trend toward decreasing levels of EXE-cys (P_{trend} = 0.0067)

TABLE 2
Major EXE metabolite concentrations in the plasma and urine of subjects taking EXE

	Plasma (nM)			Urine (nmol/mg creatinine)		
	Mean ± SE	Range	Fraction of TEM ± SE	Mean ± SE	Range	Fraction of TEM ± SE
EXE	24 ± 22	3–104	0.20 ± 0.11	0.37 ± 0.66	0.000062–3.2	0.019 ± 0.022
17β-DHE	3.3 ± 2.4	0.87–14	0.034 ± 0.024	0.011 ± 0.017	0–0.099	0.00083 ± 0.0015
17β-DHE-Gluc	50 ± 64	0.39–358	0.35 ± 0.21	2.3 ± 5.6	0.068–45	0.16 ± 0.16
EXE-cys	39 ± 37	4.3–226	0.32 ± 0.12	9.8 ± 8.9	0.0035–50	0.63 ± 0.16
17β-DHE-cys	10 ± 6.8	1.2–31	0.095 ± 0.54	2.8 ± 2.4	0.0033–10	0.19 ± 0.089

SE, standard error; TEM, total exemestane metabolites (EXE, 17β-DHE, 17β-DHE-Gluc, EXE-cys, 17β-DHE-cys).

and 17β-DHE-cys (P_{trend} = 0.028) was observed in plasma in subjects with increasing numbers of the *GSTA1*B* allele. In contrast, the relative plasma 17β-DHE-Gluc levels were significantly (P = 0.013) higher for subjects with the *GSTA1* *B*B genotype (0.47 17β-DHE-Gluc/TEM) as compared with subjects with the *GSTA1* *A*A genotype (0.30 17β-DHE-Gluc/TEM); a significant (P_{trend} = 0.00097) trend of increasing plasma 17β-DHE-Gluc levels was observed in subjects with increasing numbers of the *GSTA1*B* allele. No significant differences were observed for the levels of plasma EXE or 17β-DHE in the plasma of subjects after stratification by *GSTA1* genotype (results not shown). Additionally, no significant correlations were observed between plasma phase II EXE metabolite levels and *GSTM1* genotypes (Fig. 2B). Although the two patients with three copies of the *GSTM1* gene were not included in the association analysis of *GSTM1* genotype versus plasma or urinary EXE metabolites, their mean EXE-cys levels were 24 ± 4.8 nM and 7.1 ± 7.1 nmol per mg creatinine, respectively, which were lower than the 35 ± 26 nM and 9.2 ± 2.8 nmol per mg creatinine observed in plasma and urine, respectively, for patients who were homozygous wild-type for *GSTM1* (results not shown).

Similarly, there was a nonsignificant trend (P_{trend} = 0.060) toward decreasing levels of urinary EXE-cys in subjects with increasing numbers of the *GSTA1*B* allele (Fig. 3A), with urinary EXE-cys levels 15% lower for subjects with the *GSTA1* *B*B genotype (0.56 EXE-cys/TEM) as compared with subjects with the *GSTA1* *A*A genotype (0.66 EXE-cys/TEM). Also, similar to that observed in plasma, a significant (P = 0.026) 52% higher level of urinary 17β-DHE-Gluc was observed in subjects with the *GSTA1* *B*B genotype (0.25 17β-DHE-Gluc/TEM) as compared with subjects with the *GSTA1* *A*A genotype (0.12 17β-DHE-Gluc/TEM), and a significant (P_{trend} = 0.0089) trend in urinary 17β-DHE-Gluc

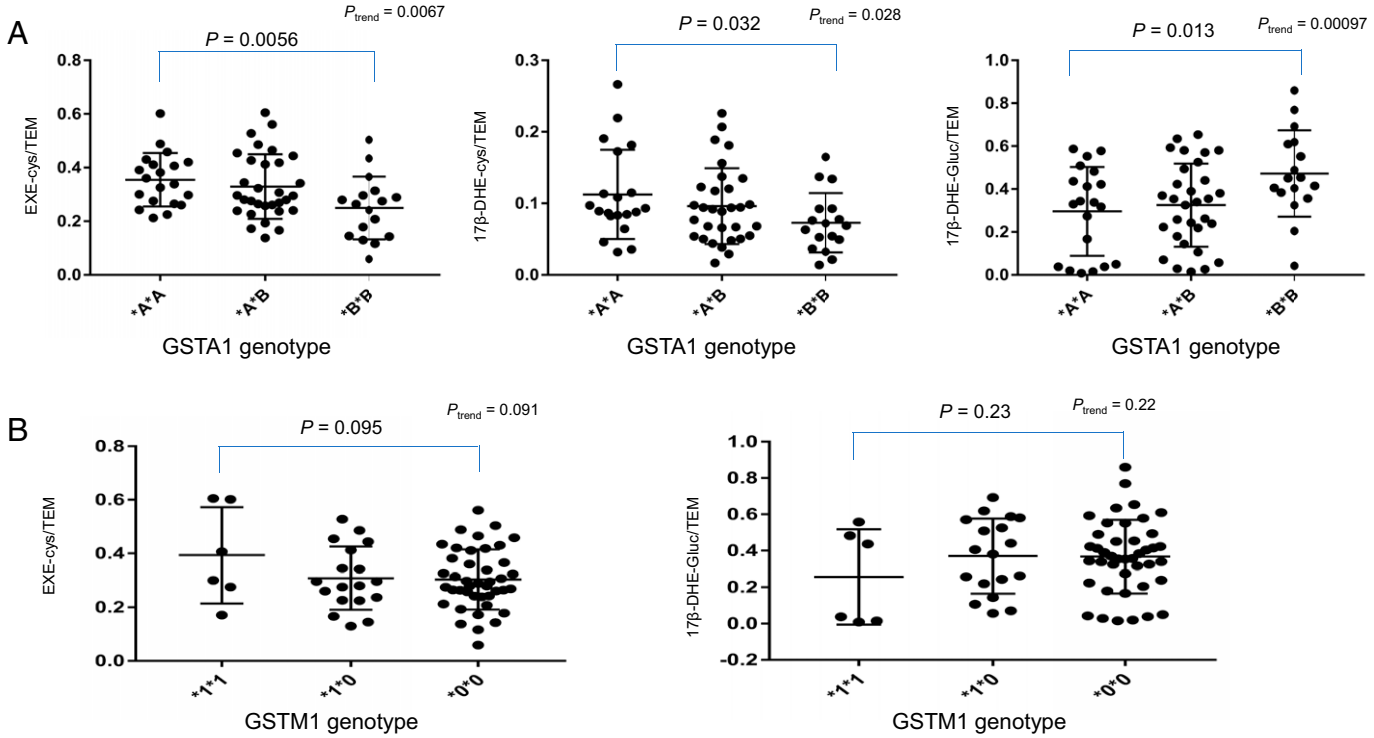

Fig. 2. Association between GST genotype and plasma EXE metabolites. The levels of EXE and its metabolites (17β-DHE, EXE-cys, 17β-DHE-cys, and 17β-DHE-Gluc) were determined in the plasma of 68 patients taking EXE, then stratified by *GSTA1* and *GSTM1* genotype. EXE and metabolite levels are presented as a fraction of total EXE + EXE metabolites (TEM = EXE + 17β-DHE + EXE-cys + 17β-DHE-cys + 17β-DHE-Gluc). (A) EXE-cys/TEM, 17β-DHE-cys/TEM and 17β-DHE-Gluc/TEM versus *GSTA1* genotype. *GSTA1*A* represents the wild type *GSTA1* allele, whereas *GSTA1**B represents polymorphic *GSTA1* allele. (B) EXE-cys/TEM and 17β-DHE-Gluc/TEM versus *GSTM1* copy number variant genotype. The *GSTM1*1* represents the wild-type gene, whereas the *GSTM1*0* corresponds to the *GSTM1* deletion variant. Since GSTM1 is not active against 17β-DHE, the 17β-DHE-cys fraction versus *GSTM1* genotype was not included in this analysis. Within each genotype, the middle bars indicate the mean, whereas the upper and lower bars represent the standard error of the mean. Statistical analysis included unpaired t test and ANOVA test for trend.

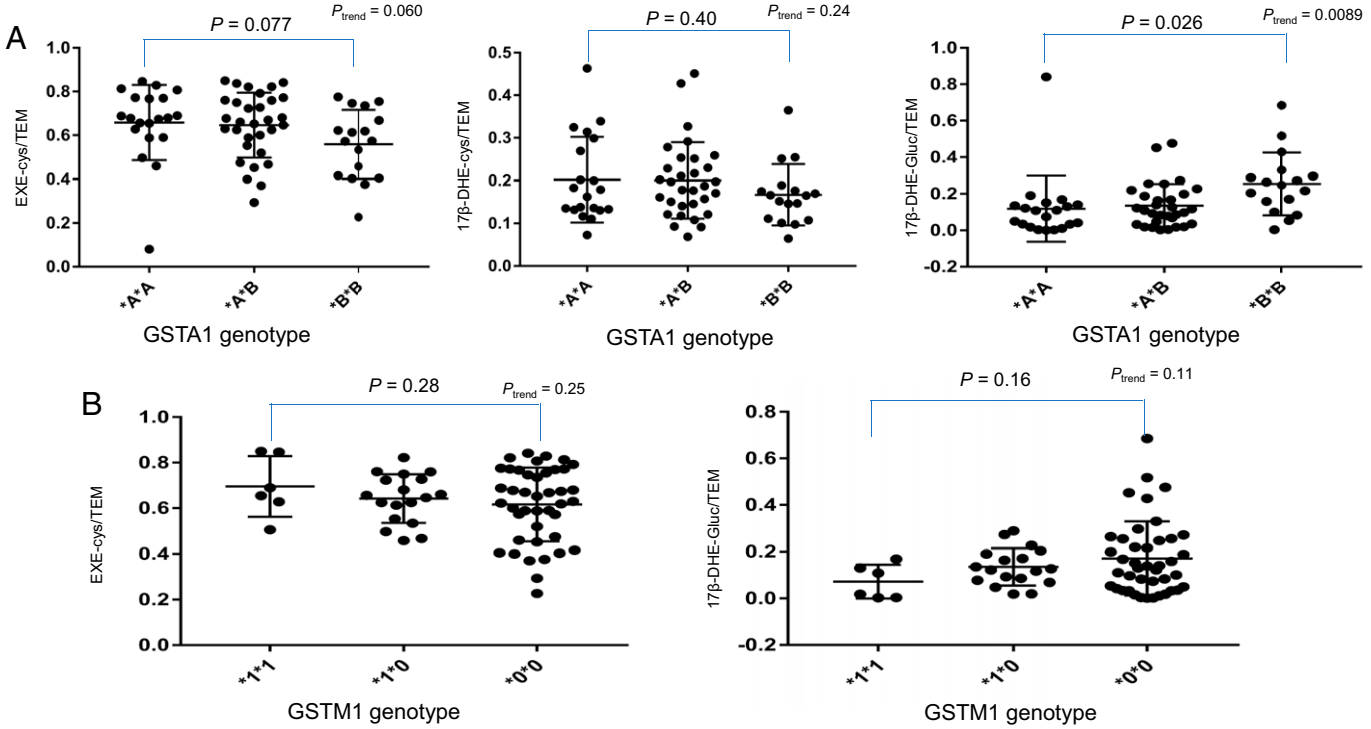

Fig. 3. Association between GST genotype and urinary EXE metabolites. The levels of EXE and its metabolites (17β-DHE, EXE-cys, 17β-DHE-cys, and 17β-DHE-Gluc) were determined in the urine of 68 patients taking EXE, then stratified by *GSTA1* and *GSTM1* genotype. EXE and metabolite levels are presented as a fraction of total EXE + EXE metabolites (TEM = EXE + 17β-DHE + EXE-cys + 17β-DHE-cys + 17β-DHE-Gluc). (A) EXE-cys/TEM, 17β-DHE-cys/TEM and 17β-DHE-Gluc/TEM versus *GSTA1* genotype. The *GSTA1*A* represents the wild type *GSTA1* allele, whereas *GSTA1*B* represents polymorphic *GSTA1* allele. (B) EXE-cys/TEM and 17β-DHE-Gluc/TEM versus *GSTM1* copy number variant genotype. The *GSTM1*1* represents the wild-type gene, whereas the *GSTM1*0* corresponds to the *GSTM1* deletion variant. Since GSTM1 is not active against 17β-DHE, the 17β-DHE-cys fraction versus *GSTM1* genotype was not included in this analysis. Within each genotype, the middle bars indicate the mean, whereas the upper and lower bars represent the standard error of the mean. Statistical analysis included unpaired *t* test and ANOVA test for trend.

levels was observed in subjects with increasing numbers of the *GSTA1*B* allele. Also, similar to the results observed in the plasma, no significant correlations were observed between urinary phase II EXE metabolite levels and *GSTM1* genotypes (Fig. 3B), and no correlation between urinary EXE, 17β-DHE, or 17β-DHE-cys levels and *GSTA1* genotype was observed (results not shown).

Discussion

Despite the increased clinical benefits of AI therapy, up to 56% of patients do not respond, with patient compliance rates low because of adverse events, such as hot flashes, fatigue, and myalgia (Paridaens et al., 2003; Paridaens et al., 2008; Goss et al., 2011; Hadji et al., 2013; Blok et al., 2018). Genetic variation in key EXE-metabolizing enzymes may be an important factor that contributes to individual variation in the metabolism, efficacy, and adverse events in patients taking EXE, and identifying pharmacogenomic factors contributing to this variation can help personalize treatment (Ingle, 2013), potentially resulting in improved compliance and patient outcomes. Previous studies have shown that the glucuronidation of the major active EXE metabolite, 17β-DHE, by UGT2B17 is an important phase II metabolic pathway for EXE (Luo et al., 2017), and that the *UGT2B17* deletion was associated with altered 17β-DHE and 17β-DHE-Gluc levels in the plasma and urine of women taking EXE (Luo et al., 2017) and influences EXE pharmacokinetics (Chen et al., 2016). However, more recent studies have shown that glutathionylation via GST enzymes is also a major phase II elimination pathway for EXE, with GSTA1 the major glutathione S-transferase involved in the hepatic metabolism of EXE and 17β-DHE (Luo et al., 2018; Teslenko et al., 2021). GST-mediated glutathione-conjugated products of EXE and 17β-DHE are further metabolized to cysteine conjugates by γ-glutamyl transferase and dipeptidases, resulting in the major EXE-cys and 17β-DHE-cys metabolites observed in the plasma and urine of patients taking EXE (Luo et al., 2018).

In the present study, we demonstrated that the *GSTA1*B* allele was associated with significant decreases in HLC GSH conjugation activity for both EXE and 17β-DHE, with a significant decrease in both EXE-cys and 17β-DHE-cys observed in specimens from subjects with the *GSTA1* *B*B genotype as compared with specimens from subjects with the *GSTA1* *A*A genotype. This pattern was also observed in the plasma of subjects taking EXE. Subjects with the *GSTA1* *B*B genotype exhibited significant decreases in plasma EXE-cys and 17β-DHE-cys levels, respectively, as compared with subjects with the *GSTA1* *A*A genotype, with statistically significant linear trends indicating decreasing levels of plasma EXE-cys and 17β-DHE-cys with increasing numbers of the *GSTA1*B* allele.

The data in the present study are consistent with previous functional studies demonstrating that the *GSTA1*B* allele is associated with decreased GSTA1 expression based on results from luciferase reporter assays (Morel et al., 2002). Previous studies demonstrated that the lower transcriptional activity

observed for the *GSTA1*B* allele was caused by the G > A substitution at the −52 location interfering with the binding of the ubiquitous transcription factor Sp1, resulting in four-fold lower *GSTA1* hepatic expression as compared with wild-type GSTA1 encoded by the *GSTA1*A* allele (Morel et al., 2002; Coles and Kadlubar, 2005a). Consistent with these previous studies, the homozygous *GSTA1* *B*B genotype was shown to be associated with the altered metabolism, efficacy, and toxicity of several agents, including cyclophosphamide, busulfan, and azathioprine (Ansari et al., 2017; Lucafò et al., 2019a; Michaud et al., 2019; Attia et al., 2021), and multiple studies have linked the *GSTA1* *B*B genotype to increased risk of colorectal, prostate, breast, and bladder cancer (Deng et al., 2015).

A similar, though nonsignificant, pattern was observed in the urine from the same subjects taking EXE, where a 15% decrease in urinary EXE-cys levels were observed in subjects with the GSTA1 *B*B genotype. This decrease is roughly 1.5-fold less than the decrease observed in plasma EXE-cys levels for the same subjects. This lack of statistical significance may be attributed to the extra-hepatic GSTM3 enzyme, which was previously shown to exhibit the highest intrinsic clearance of all GST enzymes tested against EXE in vitro (Teslenko et al., 2021). According to the human protein atlas, GSTM3 is highly expressed in the human kidney [http://www.proteinatlas.org; queried on February 20th, 2022; (Uhlén et al., 2015)]. This suggests that although this enzyme may not be playing a major role in EXE conjugation in the liver, it could be playing a more important role in kidney-related urinary metabolism. Interestingly, the *GSTM3* gene has a 3 base pair deletion polymorphism in intron 6 [resulting in the *GSTM3*B* allele (rs200126965)] with a low minor allele frequency of 2%–4% (Wang et al., 2020). GSTM3 genotyping analysis was performed in the present study, resulting in the identification of only one *A/*B heterozygote and no homozygous *GSTM3* *B/*B subjects in this population (results not shown).

Most interestingly, in contrast to the decreases observed for EXE-cys and 17β-DHE-cys, 17β-DHE-Gluc levels were significantly increased by 36%–52% in both the plasma and urine from patients with the *GSTA1* *B*B genotype. This suggests that decreases in GSTA1 conjugation lead to a corresponding shift in phase II metabolism toward the glucuronidation pathway. Given that both EXE-cys and 17β-DHE-cys are active metabolites of EXE (unpublished results), this corresponding increase in the inactive 17β-DHE-Gluc in subjects with the *GSTA1* *B*B genotype would result in decreased levels of total active EXE in these subjects.

No significant correlation between *GSTM1* genotype and either HLC EXE-GS rate of formation or EXE-cys and 17β-DHE-Gluc levels in both plasma and urine from patients taking EXE were observed in the present study. These data suggest that *GSTM1* genotype has little influence on EXE metabolism in vivo and are consistent with previous studies showing that compared with GSTA1, the GSTM1 intrinsic clearance is 2.6-fold lower, and its hepatic expression is 7.5-fold lower (Teslenko et al., 2021). Interestingly, the *GSTM1* null genotype was not in Hardy-Weinberg equilibrium in the populations examined in this study. A likely explanation is that the *GSTM1* null genotype was shown in previous studies to be associated with risk for both hepatocellular carcinoma as well as breast cancer (Qiu et al., 2016; Li et al., 2019). The higher-than-expected *GSTM1* null genotype frequency observed in the present studies is consistent with the fact that the liver specimens used in this study were originally from patients who had hepatocarcinoma, and the patients taking EXE who participated in this study were diagnosed with breast cancer.

In summary, this is the first comprehensive pharmacogenomic study to assess the effects of major GST polymorphisms on EXE metabolism both ex vivo and in patients taking EXE for ER+ breast cancer. These studies demonstrate an association with the *GSTA1*B* allele and decreases in (1) EXE-GS and 17β-DHE-GS formation in liver specimens ex vivo and (2) in EXE-cys and 17β-DHE-cys levels in vivo in patients taking EXE. Decreases in these metabolite levels also corresponded with increases in the relative levels of 17β-DHE-Gluc in patients homozygous for *GSTA1*B* allele, indicating an increased importance of the glucuronidation pathway in EXE metabolism in these individuals. Further studies evaluating the role of the *GSTA1* *B*B genotype in EXE efficacy, side effects, and overall treatment outcomes should be performed to fully elucidate the importance of this genotype in patients taking EXE.

Authorship Contributions

Participated in research design: Teslenko, Lazarus.

Conducted experiments: Teslenko, Trudeau, Luo, Chen, Truica, Lazarus.

Performed data analysis: Teslenko, Chen, Truica, Lazarus.

Wrote or contributed to the writing of the manuscript: Teslenko, Watson, Truica, Lazarus.

References

Akram M, Iqbal M, Daniyal M, and Khan AU (2017) Awareness and current knowledge of breast cancer. *Biol Res* **50**:33.

Allocati N, Masulli M, Di Ilio C, and Federici L (2018) Glutathione transferases: substrates, inihibitors and pro-drugs in cancer and neurodegenerative diseases. *Oncogenesis* **7**:8.

Ansari M, Curtis PH, Uppugunduri CRS, Rezgui MA, Nava T, Mlakar V, Lesne L, Théoret Y, Chalandon Y, Dupuis LL, et al. (2017) GSTA1 diplotypes affect busulfan clearance and toxicity in children undergoing allogeneic hematopoietic stem cell transplantation: a multicenter study. *Oncotarget* **8**:90852–90867.

Ashmore JH, Luo S, Watson CJW, and Lazarus P (2018) Carbonyl reduction of NNK by recombinant human lung enzymes: identification of HSD17β12 as the reductase important in (R)-NNAL formation in human lung. *Carcinogenesis* **39**:1079–1088.

Attia DHS, Eissa M, Samy LA, and Khattab RA (2021) Influence of glutathione S transferase A1 gene polymorphism (-69C > T, rs3957356) on intravenous cyclophosphamide efficacy and side effects: a case-control study in Egyptian patients with lupus nephritis. *Clin Rheumatol* **40**:753–762.

Blok EJ, Kroep JR, Meershoek-Klein Kranenbarg E, Duijm-de Carpentier M, Putter H, Liefers GJ, Nortier JWR, Rutgers EJT, Seynaeve CM, and van de Velde CJH (2018) Treatment decisions and the impact of adverse events before and during extended endocrine therapy in postmenopausal early breast cancer. *Eur J Cancer* **95**:59–67.

Burstein HJ, Lacchetti C, Anderson H, Buchholz TA, Davidson NE, Gelmon KA, Giordano SH, Hudis CA, Solky AJ, Stearns V, et al. (2019) Adjuvant endocrine therapy for women with hormone receptor-positive breast cancer: ASCO clinical practice guideline focused update. *J Clin Oncol* **37**:423–438.

Campos SM (2004) Aromatase inhibitors for breast cancer in postmenopausal women. *Oncologist* **9**:126–136.

Chen SM, Atchley DH, Murphy MA, Gurley BJ, and Kamdem LK (2016) Impact of UGT2B17 gene deletion on the pharmacokinetics of 17-hydroexemestane in healthy volunteers. *J Clin Pharmacol* **56**:875–884.

Coles BF and Kadlubar FF (2005a) Human alpha class glutathione S-transferases: genetic polymorphism, expression, and susceptibility to disease. *Methods Enzymol* **401**:9–42.

Coles BF and Kadlubar FF (2005b) Human Alpha Class Glutathione S-Transferases: Genetic Polymorphism, Expression, and Susceptibility to Disease, in *Methods in Enzymology* (Sies H and Packer L, eds) pp 9–42, Academic Press, Cambridge, MA.

Coombes RC, Kilburn LS, Snowdon CF, Paridaens R, Coleman RE, Jones SE, Jassem J, Van de Velde CJ, Delozier T, Alvarez I, et al.; Intergroup Exemestane Study (2007) Survival and safety of exemestane versus tamoxifen after 2-3 years' tamoxifen treatment (Intergroup Exemestane Study): a randomised controlled trial. *Lancet* **369**:559–570.

Coughtrie MW, Burchell B, and Bend JR (1987) Purification and properties of rat kidney UDP-glucuronosyltransferase. *Biochemical Pharmacology* **36**:245–251.

Dellinger RW, Chen G, Blevins-Primeau AS, Krzeminski J, Amin S, and Lazarus P (2007) Glucuronidation of PhIP and N-OH-PhIP by UDP-glucuronosyltransferase 1A10. *Carcinogenesis* **28**:2412–2418.
Deng Q, He B, Pan Y, Sun H, Liu X, Chen J, Ying H, Lin K, Peng H, and Wang S (2015) Polymorphisms of GSTA1 contribute to elevated cancer risk: evidence from 15 studies. *J BUON* **20**:287–295.
Elhasid R, Krivoy N, Rowe JM, Sprecher E, Adler L, Elkin H, and Efrati E (2010) Influence of glutathione S-transferase A1, P1, M1, T1 polymorphisms on oral busulfan pharmacokinetics in children with congenital hemoglobinopathies undergoing hematopoietic stem cell transplantation. *Pediatr Blood Cancer* **55**:1172–1179.
Geisler SA and Olshan AF (2001) GSTM1, GSTT1, and the risk of squamous cell carcinoma of the head and neck: a mini-HuGE review. *Am J Epidemiol* **154**:95–105.
Goss PE, Ingle JN, Alés-Martínez JE, Cheung AM, Chlebowski RT, Wactawski-Wende J, McTiernan A, Robbins J, Johnson KC, Martin LW, et al.; NCIC CTG MAP.3 Study Investigators (2011) Exemestane for breast-cancer prevention in postmenopausal women. *N Engl J Med* **364**:2381–2391.
Hadji P, Ziller V, Kyvernitakis J, Bauer M, Haas G, Schmidt N, and Kostev K (2013) Persistence in patients with breast cancer treated with tamoxifen or aromatase inhibitors: a retrospective database analysis. *Breast Cancer Res Treat* **138**:185–191.
Harbeck N and Gnant M (2017) Breast cancer. *Lancet* **389**:1134–1150.
Hayes JD, Flanagan JU, and Jowsey IR (2005) Glutathione transferases. *Annu Rev Pharmacol Toxicol* **45**:51–88.
Hayes JD and Strange RC (2000) Glutathione S-transferase polymorphisms and their biological consequences. *Pharmacology* **61**:154–166.
Henry NL, Azzouz F, Desta Z, Li L, Nguyen AT, Lemler S, Hayden J, Tarpinian K, Yakim E, Flockhart DA, et al. (2012) Predictors of aromatase inhibitor discontinuation as a result of treatment-emergent symptoms in early-stage breast cancer. *J Clin Oncol* **30**:936–942.
Hinchman CA and Ballatori N (1994) Glutathione conjugation and conversion to mercapturic acids can occur as an intrahepatic process. *J Toxicol Environ Health* **41**:387–409.
Ingle JN (2013) Pharmacogenomics of endocrine therapy in breast cancer. *J Hum Genet* **58**:306–312.
Jahan N, Jones C, and Rahman RL (2021) Endocrine prevention of breast cancer. *Mol Cell Endocrinol* **530**:111284.
Jannuzzo MG, Poggesi I, Spinelli R, Rocchetti M, Cicioni P, and Buchan P (2004) The effects of degree of hepatic or renal impairment on the pharmacokinetics of exemestane in postmenopausal women. Cancer Chemother Pharmacol **53**:475–481.
Josephy PD (2010) Genetic variations in human glutathione transferase enzymes: significance for pharmacology and toxicology. *Hum Genomics Proteomics* **2010**:876940.
Kamdem LK, Flockhart DA, and Desta Z (2011) In vitro cytochrome P450-mediated metabolism of exemestane. *Drug Metab Dispos* **39**:98–105.
Kieback DG, Harbeck N, Bauer W, Hadji P, Weyer G, Menschik T, and Hasenburg A (2010) Endometrial effects of exemestane compared to tamoxifen within the Tamoxifen Exemestane Adjuvant Multicenter (TEAM) trial: results of a prospective gynecological ultrasound substudy. *Gynecol Oncol* **119**:500–505.
Kittaneh M and Glück S (2011) Exemestane in the adjuvant treatment of breast cancer in postmenopausal women. *Breast Cancer (Auckl)* **5**:209–226.
Li S, Xue F, Zheng Y, Yang P, Lin S, Deng Y, Xu P, Zhou L, Hao Q, Zhai Z, et al. (2019) GSTM1 and GSTT1 null genotype increase the risk of hepatocellular carcinoma: evidence based on 46 studies. *Cancer Cell Int* **19**:76.
Loibl S, Poortmans P, Morrow M, Denkert C, and Curigliano G (2021) Breast cancer. *Lancet* **397**:1750–1769.
Lucafò M, Stocco G, Martelossi S, Favretto D, Franca R, Malusà N, Lora A, Bramuzzo M, Naviglio S, Cecchin E, et al. (2019a) Azathioprine biotransformation in young patients with inflammatory bowel disease: contribution of glutathione-S transferase M1 and A1 variants. *Genes (Basel)* **10**:277.
Lucafò M, Stocco G, Martelossi S, Favretto D, Franca R, Malusà N, Lora A, Bramuzzo M, Naviglio S, Cecchin E, et al. (2019b) Azathioprine biotransformation in young patients with inflammatory bowel disease: contribution of glutathione-S transferase M1 and A1 variants. *Genes (Basel)* **10**:277.
Luo S, Chen G, Truica C, Baird CC, Leitzel K, and Lazarus P (2017) Role of the UGT2B17 deletion in exemestane pharmacogenetics. *Pharmacogenomics J* **18**:295–300.
Luo S, Chen G, Truica CI, Baird CC, Xia Z, and Lazarus P (2018) Identification and quantification of novel major metabolites of the steroidal aromatase inhibitor, exemestane. *Drug Metab Dispos* **46**:1867–1878.
Michaud V, Tran M, Pronovost B, Bouchard P, Bilodeau S, Alain K, Vadnais B, Franco M, Bélanger F, and Turgeon J (2019) Impact of *GSTA1* polymorphisms on busulfan oral clearance in adult patients undergoing hematopoietic stem cell transplantation. *Pharmaceutics* **11**:440.
Mikstacki A, Skrzypczak-Zielinska M, Zakerska-Banaszak O, Tamowicz B, Skibinska M, Molinska-Glura M, Szalata M, and Slomski R (2016) Impact of CYP2E1, GSTA1 and GSTP1 gene variants on serum alpha glutathione S-transferase level in patients undergoing anaesthesia. *BMC Med Genet* **17**:40.
Morel F, Rauch C, Coles B, Le Ferrec E, and Guillouzo A (2002) The human glutathione transferase alpha locus: genomic organization of the gene cluster and functional characterization of the genetic polymorphism in the hGSTA1 promoter. *Pharmacogenetics* **12**:277–286.
Paridaens R, Dirix L, Lohrisch C, Beex L, Nooij M, Cameron D, Biganzoli L, Cufer T, Duchateau L, Hamilton A, et al.; European Organization for the Research and Treatment of Cancer (EORTC)- Investigational Drug Branch for Breast Cancer (IDBBC) (2003) Mature results of a randomized phase II multicenter study of exemestane versus tamoxifen as first-line hormone therapy for postmenopausal women with metastatic breast cancer. *Ann Oncol* **14**:1391–1398.
Paridaens RJ, Dirix LY, Beex LV, Nooij M, Cameron DA, Cufer T, Piccart MJ, Bogaerts J, and Therasse P (2008) Phase III study comparing exemestane with tamoxifen as first-line hormonal treatment of metastatic breast cancer in postmenopausal women: the European Organisation for Research and Treatment of Cancer Breast Cancer Cooperative Group. *J Clin Oncol* **26**:4883–4890.
Perera FP, Mooney LA, Stampfer M, Phillips DH, Bell DA, Rundle A, Cho S, Tsai W-Y, Ma J, Blackwood A, et al.; Physicians' Health Cohort Study (2002) Associations between carcinogen-DNA damage, glutathione S-transferase genotypes, and risk of lung cancer in the prospective Physicians' Health Cohort Study. *Carcinogenesis* **23**:1641–1646.
Peterson A, Xia Z, Chen G, and Lazarus P (2017) In vitro metabolism of exemestane by hepatic cytochrome P450s: impact of nonsynonymous polymorphisms on formation of the active metabolite 17β-dihydroexemestane. *Pharmacol Res Perspect* **5**:e00314.
Platt A, Xia Z, Liu Y, Chen G, and Lazarus P (2016) Impact of nonsynonymous single nucleotide polymorphisms on in-vitro metabolism of exemestane by hepatic cytosolic reductases. *Pharmacogenet Genomics* **26**:370–380.
Qiu Z, Wilson RS, Liu Y, R Dun A, Saleeb RS, Liu D, Rickman C, Frame M, Duncan RR, and Lu W (2016) Translation microscopy (TRAM) for super-resolution imaging. *Sci Rep* **6**:19993.
Sun D, Chen G, Dellinger RW, Sharma AK, and Lazarus P (2010) Characterization of 17-dihydroexemestane glucuronidation: potential role of the UGT2B17 deletion in exemestane pharmacogenetics. *Pharmacogenet Genomics* **20**:575–585.
Suvakov S, Damjanovic T, Pekmezovic T, Jakovljevic J, Savic-Radojevic A, Pljesa-Ercegovac M, Radovanovic S, Simic DV, Pljesa S, Zarkovic M, et al. (2014) Associations of GSTM1*0 and GSTA1*A genotypes with the risk of cardiovascular death among hemodialyses patients. *BMC Nephrol* **15**:12.
Teslenko I, Watson CJW, Xia Z, Chen G, and Lazarus P (2021) Characterization of cytosolic glutathione *S*-transferases involved in the metabolism of the aromatase inhibitor, exemestane. *Drug Metab Dispos* **49**:1047–1055.
Uhlén M, Fagerberg L, Hallström BM, Lindskog C, Oksvold P, Mardinoglu A, Sivertsson Å, Kampf C, Sjöstedt E, Asplund A, et al. (2015) Proteomics. tissue-based map of the human proteome. *Science* **347**:1260419.
Valle M, Di Salle E, Jannuzzo MG, Poggesi I, Rocchetti M, Spinelli R, and Verotta D (2005) A predictive model for exemestane pharmacokinetics/pharmacodynamics incorporating the effect of food and formulation. *Br J Clin Pharmacol* **59**:355–364.
Vianna-Jorge R, Festa-Vasconcellos JS, Goulart-Citrangulo SMT, and Leite MS (2013) Functional polymorphisms in xenobiotic metabolizing enzymes and their impact on the therapy of breast cancer. *Front Genet* **3**:329.
Wang S, Yang J, You L, Dai M, and Zhao Y (2020) GSTM3 function and polymorphism in cancer: emerging but promising. *Cancer Manag Res* **12**:10377–10388.
Yokota H, Ohgiya N, Ishihara G, Ohta K, and Yuasa A (1989) Purification and properties of UDP-glucuronyltransferase from kidney microsomes of β-naphthoflavone-treated rat. *The Journal of Biochemistry* **106**:248–252.
Zelnak AB and O'Regan RM (2015) Optimizing endocrine therapy for breast cancer. *J Natl Compr Canc Netw* **13**:e56–e64.

Address correspondence to: Dr. Philip Lazarus, Department of Pharmaceutical Sciences, College of Pharmacy and Pharmaceutical Sciences, Washington State University, 412 E Spokane Falls Boulevard, Spokane, WA. E-mail: phil.lazarus@wsu.edu